



# Photo-Degradation of Phenol Using TiO<sub>2</sub>/CMK-3 Photo-Catalyst Under Medium Pressure UV Lamp

Alireza Rahmani<sup>1</sup>, Hadi Rahimzadeh<sup>1,2\*</sup>, Somayeh Beirami<sup>2</sup>

<sup>1</sup>Department of Environmental Health Engineering, Faculty of Health, Hamedan University of Medical Sciences, Hamedan, Iran

<sup>2</sup>Department of Environmental Health Engineering, Faculty of Health and Environmental Health Research Center, Golestan University of Medical Sciences, Gorgan, Iran

## \*Correspondence to

Hadi Rahimzadeh,  
Tel. +98 9112750640,  
Email: hadi\_rahimzadeh@  
yahoo.com,

Published online 20 June,  
2018



## Abstract

Phenol is considered as one of the major environmental concerns due to its characteristics including chronic toxicity, biological stability, and increasing the toxicological intermediates after biological degradation. Therefore, the aim of this study was to evaluate the photo-degradation of phenol using the titanium dioxide (TiO<sub>2</sub>) photo-catalyst on ordered mesoporous carbon (CMK-3) support under UV irradiation. In this study, the effects of some parameters including pH value (4, 5, 6, 7, 8, 9, 10), TiO<sub>2</sub>/CMK-3 concentration (0.05, 0.1, 0.15, 0.3, 0.5 g/L), irradiation time (30, 60, 90, 120, 150 min), and phenol concentration (50, 100, 150 and 200 mg/L) were assessed. The properties of the CMK-3 and TiO<sub>2</sub>/CMK-3 were compared using the transmission electron microscopy (TEM), X-ray powder diffraction (XRD) and N<sub>2</sub> adsorption-desorption isotherm. The results revealed that the process studied was remarkably affected by the parameters, and the optimum values of the parameters were as follows: pH=6, TiO<sub>2</sub>/CMK-3 concentration =0.15 g/L, phenol concentration = 100 mg/L, and irradiation time=150 min. The phenol degradation efficiency and total organic carbon (TOC) removal efficiency for phenol were 96% and 74%, respectively. Moreover, the stability greater than 7 times for the studied photo-catalyst was indicative of its high potential to be used in photo-degradation processes for the elimination of pollutants.

**Keywords:** TiO<sub>2</sub>/CMK-3, Photocatalytic degradation, Phenol, UV irradiation

Received February 6, 2018; Revised April 10, 2018; Accepted May 8, 2018

## 1. Introduction

Phenol (C<sub>6</sub>H<sub>5</sub>OH) is an aromatic organic compound which is released during various industries and processes, including coal conversion processes, coke ovens, petroleum refineries, phenolic resin manufacturing, herbicide manufacturing, fiberglass fabrication, and petrochemicals. Due to its toxicity and low biodegradability, phenol is considered as one of the major concerns for the environment, especially aquatic environments (1,2). The characteristics of phenol such as chronic toxicity, biological stability, and increasing the toxicological intermediates after biological degradation has led to its classification as a priority pollutant (3,4). Review of the previous literature has shown that this compound can affect the central nervous system and the digestive tract and can lead to skin irritation (5,6). In addition, it has been reported that intake of 8-15 mg of phenol leads to death, to such a degree that various regulations and limits have been established for phenol by the related agencies. For example, the Environmental Protection Agency (EPA) and Institute of Standards and Industrial Research of Iran have introduced 1 mg/L and 0.5 µg/L, as the maximum

allowable amounts for this compound, respectively (7,8). On this basis, elimination of phenol seems to be imperative in order to protect the life cycle.

Among various technologies suggested for elimination of phenol, the advanced oxidation processes (AOPs) using hydroxyl radical (E = 2.8 V) have been introduced as successful techniques in which the organic pollutants are completely degraded and converted into minerals, CO<sub>2</sub> and H<sub>2</sub>O (6,9). Currently, the heterogeneous photocatalysis, as one of the AOP techniques, has attracted the attention of scientists to degrade the various types of pollutants. This technique is based on the use of a light source, a semiconductor photo-catalyst and an oxidizing agent (10,11). Among the photo-catalysts used in this process, the TiO<sub>2</sub>-based photo-catalytic materials has the exceptional properties including the complete removal of organic pollutants, low cost, and chemical stability and non-toxicity (12,13). Despite outstanding properties of TiO<sub>2</sub>, its deficiencies including the hard separation of TiO<sub>2</sub> nanoparticles from the solution and the tendency to accumulate in high concentrations limit its applications (14,15).

The development of  $\text{TiO}_2$  support has been recently considered in the studies for the enhancement of efficiency of  $\text{TiO}_2$  and in this regard, various supports have been introduced and used (16-19). The activated carbon was identified as one of the best supports for  $\text{TiO}_2$  and used in various photo-degradation studies to remove the phenol (20), tetracycline (21), dye (22) and so on. Special properties of the activated carbon, for example, excellent surface area, well-developed pore structure, and high adsorption capacity were the reasons for its application as the support in various studies; however, some issues associated with the use of this substance, such as decreasing the process efficiency has motivated the scientists to discover new substances for the support of photo-catalysts (23-25). The ordered mesoporous carbons are one of these substances which have been studied in photo-degradation processes. The ordered mesoporous carbon has a hexagonal two-dimensional structure and is produced by the carbonization of silica mesoporous substances such as uniform pore size SBA-15 (25,26). The high surface area, large pore volume, high-purity synthesis, high physical and chemical stability in environmental fields, and energy storage are the characteristics of the ordered mesoporous carbon that give the possibility to be used as a successful support (27). Previous studies have revealed the successful use of CMK-3 in the removal of pollutants; for example, Hu et al utilized the Fe/CMK-3 for photo-degradation of the phenol and found that it has a suitable ability for adsorption and oxidation of the phenol and can easily be separated from the solution with minimal leaching (28).

The aim of this study was to evaluate the photo-catalytic degradation of phenol by  $\text{TiO}_2$  photo-catalyst on ordered mesoporous carbon (CMK-3) support under medium pressure UV irradiation. In addition, the effect of different parameters such as pH value, catalyst concentration, phenol concentration, and irradiation time was studied. Moreover, the stability and reusability of  $\text{TiO}_2$ /CMK-3 catalyst were investigated in 7 consecutive cycles under optimum conditions.

## 2. Materials and Methods

Tetraethyl orthosilicate (TEOS, 98%), titanium (IV) isopropoxide (TIP 97%) and Pluronic P123 (EO20PO70EO20) were purchased from Sigma-Aldrich CO., USA. Other chemicals including sucrose, sodium hydroxide (NaOH), ethanol, sulfuric acid ( $\text{H}_2\text{SO}_4$ , 98%), and isopropyl alcohol were provided by Merck CO., Germany. All the mentioned chemicals were of analytical grade. In addition, deionized double-distilled water was utilized for all of the experiments.

### 2.1. Preparation of SBA-15, CMK-3 and $\text{TiO}_2$ /CMK-3

#### 2.1.1. Preparation of SBA-15

The synthesis of ordered mesoporous silica SBA-15, as the template for the synthesis of CMK-3, was performed

based on the previous study (29). The procedure of the SBA-15 synthesis is as follows: after dissolving 2 g P123 in 60 mL of 2M HCl solution, 15 mL deionized water at 40°C and 4.25 g of TEOS were added. Then, it was magnetically stirred at 40°C for 24 hours and the mixture was autoclaved at 100°C for 48 hours. Afterward, 0.45  $\mu\text{m}$  Whatman filter was used to recover the resultant. Then, it was initially rinsed several times with distilled water and ethanol (25%) and was finally washed with distilled water. Afterward, calcinations of filtrated solids were performed at 550°C in the air at a ramping rate of 1°C/min and kept at this temperature for 12 hours to eliminate the organic template of P123.

#### 2.1.2. Preparation of CMK-3

The preparation of CMK-3 was done according to the study of Jun et al (30). SBA-15 was used as a hard template. Initially, 1 g of SBA-15 was added to a solution obtained by dissolving 1.25 g sucrose and 0.14 g  $\text{H}_2\text{SO}_4$  (98%) in 5 mL  $\text{H}_2\text{O}$ . The resulting mixture was placed in the oven at 100°C for 6 hours. The oven temperature was later increased to 160°C for further 6 hours. In order to obtain fully polymerized and carbonized sucrose inside the pores of the silica template, 0.8 g of sucrose, 0.09 g of  $\text{H}_2\text{SO}_4$ , and 5 mL of water were again added to the pretreated sample and the mixture was then subjected to the thermal treatment as described above. The composite was then pyrolyzed in a nitrogen flow (purity = 99.999%) at 900°C and kept under these conditions for 6 h for carbonization of the polymer. The mesoporous carbon (CMK-3) was obtained by eliminating the silica template using a 1 M aqueous ethanolic NaOH solution (50 vol.% NaOH solution and 50 vol.% ethanol) twice at room temperature followed by filtration, washing, and drying at 120°C for 4 hours.

#### 2.1.3. Preparation of $\text{TiO}_2$ /CMK-3

In order to prepare  $\text{TiO}_2$ /CMK-3 with 5 wt% of  $\text{TiO}_2$ , the solution of 5.95 mL isopropyl alcohol and 0.19 mL titanium (IV) isopropoxide were added into 1.0 g of CMK-3, and then  $\text{TiO}_2$  particles were prepared by placing in an oven at 100°C with water vapor for 6 hours. The resultant was finally calcined at 700°C for 2 hours in the argon atmosphere.

## 2.2. Characterization Methods

XRD patterns of the resultant material were collected using a Philips PW 1730 X-ray diffractometer. The diffractograms were recorded in the  $2\theta$  range of 0.5–5° with a  $2\theta$  step size of 0.05°. The specific surface area of the  $\text{TiO}_2$ /CMK-3 was calculated according to the Brunauer–Emmet–Teller method, and the pore size distribution curves were obtained from the analysis of nitrogen adsorption isotherms using Barrett–Joyner–Halenda method on a BELSORP MINI II at -196°C (77 K). Before each measurement, the sample was heated under vacuum

at 450°C. Transmission electron microscopy (TEM) images for determination of TiO<sub>2</sub>/CMK-3 dispersion and morphology of samples were obtained using a Zeiss EM900.

### 2.3. Photo-Degradation Experiments

In this study, the photo-catalytic degradation of phenol using the TiO<sub>2</sub>/CMK-3 photo-catalyst was investigated under medium pressure UV lamp in a photo-catalytic reactor at room temperature. The light source was a 150-W medium pressure mercury UV lamp. The 0.1N HCl and/or 0.1N NaOH was used to adjust the initial pH of the solution. This study was conducted under the following conditions: the initial pH values of 4, 5, 6, 7, 8, 9, 10; TiO<sub>2</sub>/CMK-3 concentrations of 0.05, 0.1, 0.15, 0.3, 0.5 g/L; irradiation times of 30, 60, 90, 120, 150 minutes; and phenol concentrations of 50, 100, 150 and 200 mg/L. In each experiment, the certain amount of photo-catalyst was added into 150 mL of phenol solution under magnetic stirring and maintained in dark condition for 60 minutes in order to reach the adsorption equilibrium, and then the suspension was irradiated under UV light. Afterward, approximately 5 mL of the suspension sample was withdrawn at the predetermined time interval and separated by centrifugation at 2000 rpm for 4 minutes to achieve a clear supernatant for analysis of the concentrations of the solutes. The concentration of phenol in the supernatant was analyzed using a UV spectrophotometer (6305 UV/Vis Jenway spectrophotometer, UK) with the wavelength at 270 nm. To determine the mineralization level, the measurement of total organic carbon (TOC) was made using a TOC analyzer (Analytic Jena multi N/C 3100, Germany). All the experiments were carried out for three times and were expressed in terms of arithmetic means. The analysis was based on the removal efficiency using Eq. (1):

$$\text{Removal \%} = \left[ \frac{(\text{concentration})_0 - (\text{concentration})_t}{(\text{concentration})_0} \right] \times 100 \quad (1)$$

where (concentration)<sub>0</sub> and (concentration)<sub>t</sub> denote phenol and TOC concentrations before and after the photocatalytic reaction, respectively.

## 3. Results and Discussion

### 3.1 Characteristics of Catalyst

Low angle XRD patterns for CMK-3 and TiO<sub>2</sub>/CMK-3 are shown in Fig. 1. The ordered mesoporous carbon CMK-3 was obtained by the hard template method from SBA-15, indicating that CMK-3 is an exact replica of SBA-15. CMK-3 and TiO<sub>2</sub>/CMK-3 exhibit three peaks for 100, 110, and 200 reflections at 2θ less than 2°, corresponding to the well-defined 2D hexagonal structure. As it is evident from Fig. 1, approximately, there is no change in the XRD pattern, except for the gradual decrease in the diffraction intensity of TiO<sub>2</sub>/CMK-3, compared to CMK-3 (25).

Fig. 2 shows the N<sub>2</sub> adsorption-desorption isotherm

for CMK-3 and TiO<sub>2</sub>/CMK-3 samples at 77°K. It can be observed that the adsorption isotherm of both samples was indicative of the IV isotherm type of the mesoporous material according to the IUPAC classification. Table 1 shows the determined textural properties of the nitrogen physisorption analysis. According to this table, the values of total pore volume (V<sub>t</sub>), specific surface area (S<sub>BET</sub>), and pore size (d<sub>0</sub>) of the TiO<sub>2</sub>/CMK-3 decreased compared to CMK-3. This decrease was due to the filling of CMK-3 pores by TiO<sub>2</sub> nanoparticles.

The TEM images of CMK-3 and TiO<sub>2</sub>/CMK-3 are shown in Fig. 3. TEM images reveal that both of them are present as a short rod-like morphology. Fig. 3b confirms that the structured order of TiO<sub>2</sub>/CMK-3 is maintained even after introducing the TiO<sub>2</sub> nanoparticles into the

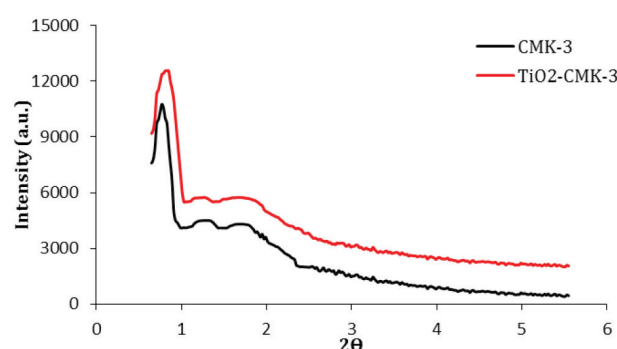


Fig. 1. Small-Angle XRD Patterns of CMK-3 and TiO<sub>2</sub>/CMK-3

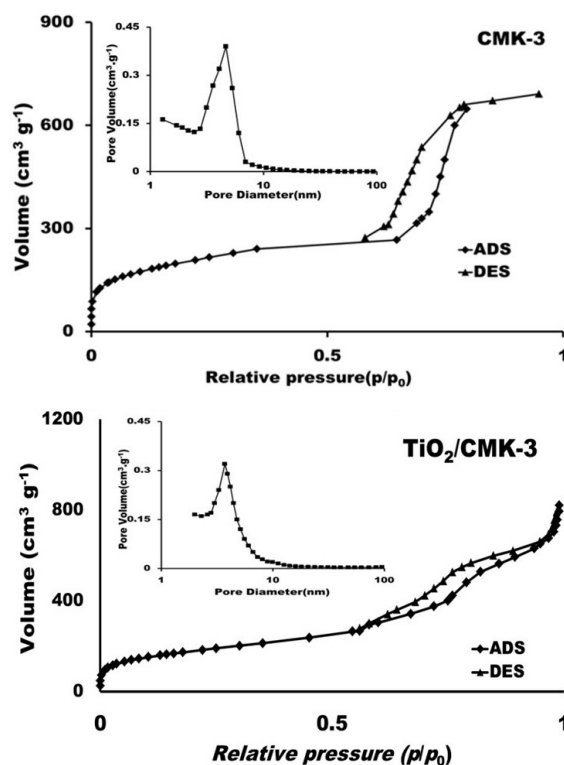


Fig. 2. Nitrogen Adsorption-Desorption Isotherms and Pore-Size Distribution (PSD) for CMK-3 and TiO<sub>2</sub>/CMK-3

**Table 1.** Textural Properties of CMK-3 and TiO<sub>2</sub>/CMK-3 Catalysts

Sample	S <sub>BET</sub> (m <sup>2</sup> g <sup>-1</sup> )	V <sub>meso</sub> <sup>a</sup> (cm <sup>3</sup> g <sup>-1</sup> )	V <sub>micro</sub> (cm <sup>3</sup> g <sup>-1</sup> )	d <sub>0</sub> (nm)
CMK-3	940.82	0.78	0.024	4.85
TiO <sub>2</sub> /CMK-3	875.8	0.69	0.016	3.65

CMK-3 channels. The TiO<sub>2</sub> nanoparticles appear as dark dot-like objects on the mesopores.

### 3.2. Photo-Catalytic Activity of TiO<sub>2</sub>/CMK-3

Before the photocatalytic experiments, a series of batch tests were conducted to accomplish the adsorption-desorption equilibrium behavior between CMK-3, TiO<sub>2</sub>/CMK-3, and phenol under dark condition. As can be seen from Fig. 4, phenol adsorption efficiencies by CMK-3 and TiO<sub>2</sub>/CMK-3 were 23.4% and 18.6%, respectively. However, higher efficiencies were obtained in the photocatalytic processes. It was also observed

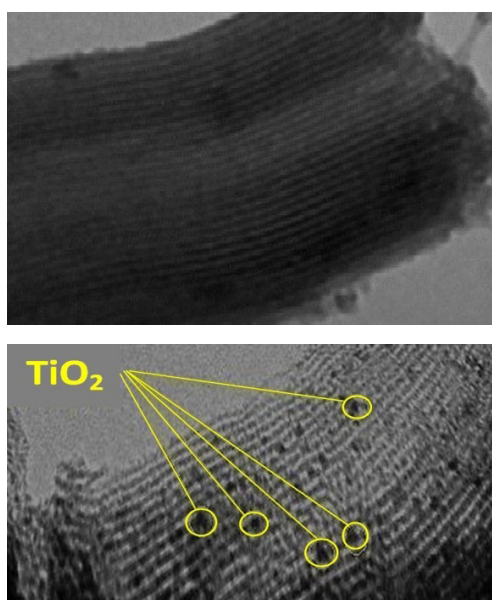


**Fig. 3.** TEM Images of the Synthesized CMK-3 and TiO<sub>2</sub>/CMK-3.

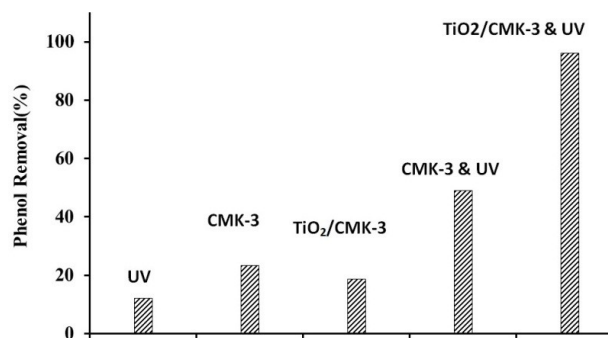


**Fig. 4.** Removal of Phenol Under Various Conditions (reaction conditions: pH= 6.0, catalyst (CMK-3 and TiO<sub>2</sub>/CMK-3) concentration = 0.15 g/L, phenol concentration =100 mg/L, and reaction time=150 min).

that TiO<sub>2</sub>/CMK-3 was more successful than CMK-3 in removing the phenol in the photocatalytic processes. Finally, photocatalytic properties of TiO<sub>2</sub>/CMK-3 in phenol removal was confirmed. Since the photocatalytic degradation of phenol is dependent on the initial solution pH values, the initial concentration of phenol, and the concentrations of catalysts, the influence of these parameters on the degradation of phenol in photocatalytic reactions was investigated.

### 3.3. The Effect of Initial pH

The effect of pH, as an important parameter affecting the photo-catalytic process, was studied at different values of 4-10 and constant conditions of other parameters (Fig. 5). As can be observed, the best results for phenol degradation were obtained at the pH values between 4 and 6, which can be described by the photo-catalytic oxidation and adsorption properties. Since the charge zero point (Pzc) of TiO<sub>2</sub>/CMK-3 is equal to 6.3, at the pH values from 4 to 6, the surface of photo-catalyst is positively charged, which results in more adsorption of the negatively charged phenol molecules on the surface of photo-catalyst and more possibility of degradation of adsorbed molecule on the surface of the photo-catalyst in the studied photo-catalytic process (10). Moreover, the presence of high volumes of holes in acidic pH increases the amount of phenol decomposition (31). These results are also confirmed by Lam et al (32).

### 3.4. Effect of catalyst concentration

The effect of catalyst concentration was studied using the TiO<sub>2</sub>/CMK-3 concentrations in the range of 0.05 to 0.5 g/L under the constant values of other parameters (the

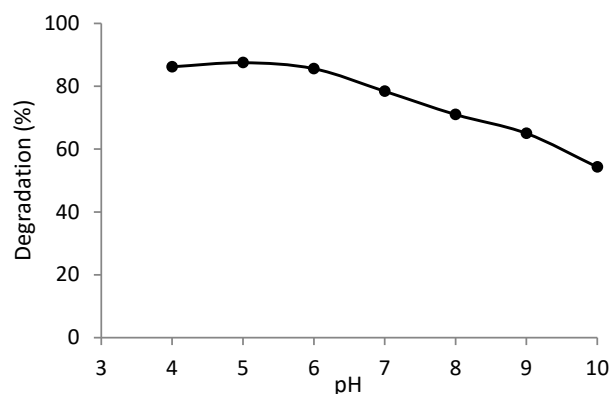


**Fig. 5.** Effect of Initial pH on the Phenol Degradation Efficiency (concentration of TiO<sub>2</sub>/CMK-3= 0.15 g/L, phenol concentration =100 mg/L, and irradiation time = 150 min).

results are presented in Fig. 6). As can be seen, the photo-catalytic activity of the studied catalyst was increased from 0.05 g/L to 0.15 g/L. Increasing the active sites on the photo-catalyst surface for the adsorption and oxidation of the phenol by the production of active radicals was reported as the cause of this event (12). However, the activity of this photo-catalyst reduced in greater concentrations (>0.2 g/L); this can be explained by the scattering of the light and the accumulation of particles by collision (10). The studies of Chiou and Juang (33) and Jiang et al confirm the obtained results (34).

### 3.5. Effect of Initial Concentration of Phenol

The effect of initial concentration of phenol was studied by varying its concentration between 50 mg/L and 200 mg/L (the obtained results are represented in Fig. 7). As illustrated, the phenol degradation efficiency was diminished by increasing its initial concentration. By increasing the initial concentration of the phenol, the number of phenol molecules on the surface of the photo-catalyst is increased and, as a result, the surface sites of the photo-catalyst is deactivated and higher amount of oxidizing agents is consumed, leading to a decrease in the

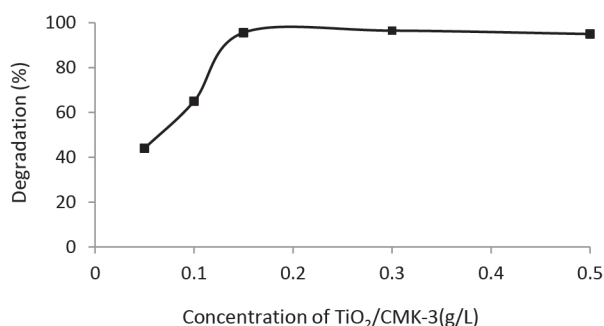


**Fig. 6.** Effect of Initial Concentration of TiO<sub>2</sub>/CMK-3 on the Phenol Degradation Efficiency (pH=6, phenol concentration=100 mg/L, and irradiation time =150 min).

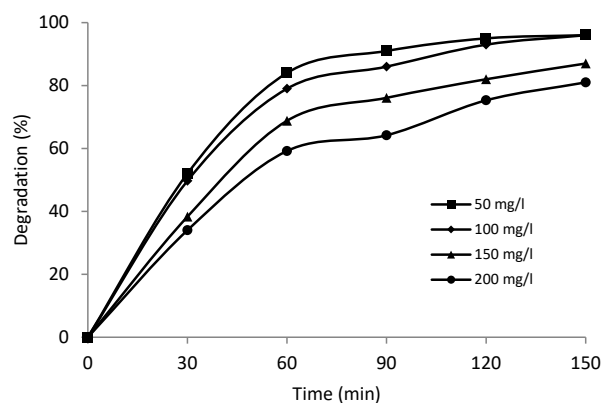


**Fig. 7.** Effect of initial concentration of phenol on the degradation efficiency of phenol (pH=6, concentration of TiO<sub>2</sub>/CMK-3=0.15 g/L, and irradiation time=150 min)

degradation efficiency (35). These results are in agreement with the results obtained by Akbal (36), Mangrulkar et al (37) and Kansal et al (38).

In addition, as can be seen in Table 2, the degradation kinetics was investigated based on the first kinetic model ( $\ln(C_0/C) = Kt$ ) for different concentrations of the phenol. Considering this table, it is observed that kinetic constant rate decreases by increasing the initial concentration of phenol, which can be due to the probability of interaction between the phenol molecules and active radicals (39).

### 3.6. Mineralization of Phenol

To study the mineralization rate of the phenol in the studied system, the TOC removal efficiency was determined. As can be observed in Fig. 8, increasing the irradiation time develops the mineralization efficiency of phenol. Increasing the probability of photo-catalytic degradation of organic compounds by oxidants produced on the TiO<sub>2</sub>/CMK-3 surface was mentioned as the reason for the increased TOC removal. Rafiee et al also observed the same results in their study when they investigated the photo-catalytic degradation of phenol (39). It was observed that the TOC removal efficiency was less than the phenol degradation efficiency, which was related to intermediate products produced in the catalytic reaction.

### 3.7. The Stability of TiO<sub>2</sub>/CMK-3

In the present study, the stability of TiO<sub>2</sub>/CMK-3 catalyst was also studied in 7 consecutive runs (the results are presented in Fig. 9). In order to study the stability of TiO<sub>2</sub>/CMK-3 photo-catalyst, the catalyst, after each run of experiment, was separated from the solution, washed with distilled water, and then dried at 60°C in an oven.

**Table 2.** Kinetic Constants for the Photo-Catalytic Degradation of Various Concentrations of Phenol

Phenol Concentration	k/min <sup>-1</sup>	R <sup>2</sup>
50	0.0223	0.9626
100	0.0213	0.9927
150	0.0135	0.9689
200	0.0108	0.9804

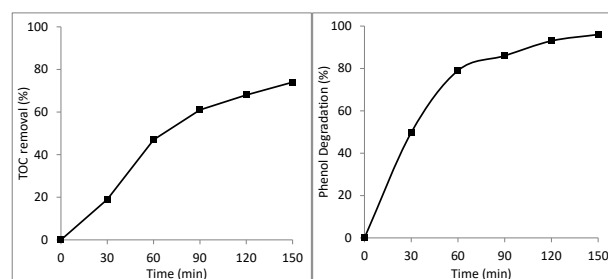


**Fig. 8.** Removal of TOC and Phenol During Photo-Catalytic Process (pH=6, TiO<sub>2</sub>/CMK-3 concentration=0.15 g/L, phenol concentration =100 mg/L)

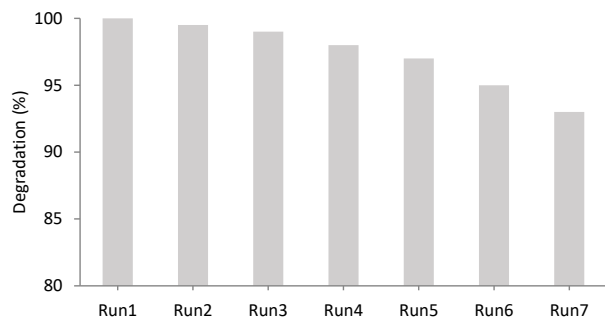


**Fig. 9.** Phenol degradation in consecutive runs using regenerated composite  $\text{TiO}_2/\text{CMK-3}$  as photo-catalyst (pH=6, concentration of  $\text{TiO}_2/\text{CMK-3}$ =0.15 g/L, phenol concentration=100 mg/L, and irradiation time=150 min)

Afterward, it was regenerated to be utilized in the next run. According to Fig. 8, the phenol removal efficiency was reduced to 95% after 5 consecutive runs, demonstrating an insignificant reduction in the catalytic activity of  $\text{TiO}_2/\text{CMK-3}$ . This proves the high stability and reusability of this catalyst (40). Moreover, the slight fall in the phenol degradation efficiency is attributed to a decrease in the photo-catalyst concentration by filtration and washing in the regeneration process. Similar results were observed by Jiang et al for the degradation of methylene orange dye using  $\text{TiO}_2/\text{carbon nanotubes}$  photo-catalyst (34).

#### 4. Conclusion

In this study, the potential of  $\text{TiO}_2/\text{CMK-3}$  photo-catalyst in the photo-catalytic degradation of phenol was studied. Analyses of XRD, TEM, and  $\text{N}_2$  adsorption-desorption revealed that  $\text{TiO}_2$  was successfully incorporated into the CMK-3 structure. The photo-catalytic degradation efficiency of phenol was robustly influenced by pH value, catalyst concentration, initial concentration of phenol, and irradiation time. The optimum conditions for the parameters studied were as follows: pH=6,  $\text{TiO}_2/\text{CMK-3}$  concentration=0.15 g/L, phenol concentration=100 mg/L, and irradiation time=150 minutes. The phenol degradation efficiency was obtained to be 96% and the TOC removal efficiency was observed to be 74%. A stability greater than 7 times for  $\text{TiO}_2/\text{CMK-3}$  photo-catalyst showed that it can be considered as a suitable photo-catalyst in photo-degradation processes.

#### Conflict of Interest Disclosures

The authors declare that they have no conflict of interests.

#### Acknowledgements

The authors announce their appreciation and gratitude to the Golestan University of Medical Sciences, for supporting this project.

#### References

- Dargahi A, Mohammadi M, Amirian F, Karami A, Almasi A. Phenol removal from oil refinery wastewater using anaerobic stabilization pond modeling and process optimization using

response surface methodology (RSM). *Desalination Water Treat.* 2017;87:199-208.

- Pradeep NV, Anupama S, Navya K, Shalini HN, Idris M, Hampannavar US. Biological removal of phenol from wastewaters: a mini review. *Applied Water Science.* 2015;5(2):105-12. doi: [10.1007/s13201-014-0176-8](https://doi.org/10.1007/s13201-014-0176-8).
- Chen Y, Yan J, Ouyang D, Qian L, Han L, Chen M. Heterogeneously catalyzed persulfate by CuMgFe layered double oxide for the degradation of phenol. *Appl Catal A Gen.* 2017;538:19-26. doi: [10.1016/j.apcata.2017.03.020](https://doi.org/10.1016/j.apcata.2017.03.020).
- Vaiano V, Matarangolo M, Murcia JJ, Rojas H, Navio JA, Hidalgo MC. Enhanced photocatalytic removal of phenol from aqueous solutions using ZnO modified with Ag. *Appl Catal B.* 2018;225:197-206. doi: [10.1016/j.apcatb.2017.11.075](https://doi.org/10.1016/j.apcatb.2017.11.075).
- Mukherjee M, Goswami S, Banerjee P, Sengupta S, Das P, Banerjee PK, et al. Ultrasonic assisted graphene oxide nanosheet for the removal of phenol containing solution. *Environ Technol Innov.* 2017. doi: [10.1016/j.eti.2016.11.006](https://doi.org/10.1016/j.eti.2016.11.006).
- Cordova Villegas LG, Mashhadi N, Chen M, Mukherjee D, Taylor KE, Biswas N. A short review of techniques for phenol removal from wastewater. *Curr Pollution Rep.* 2016;2(3):157-67. doi: [10.1007/s40726-016-0035-3](https://doi.org/10.1007/s40726-016-0035-3).
- Bazrafshan E, Biglari H, Mahvi AH. Performance evaluation of electrocoagulation process for phenol removal from aqueous solutions. *Fresen Environ Bull.* 2012;21(2):364-71.
- Afsharnia M, Saeidi M, Zarei A, Narooie MR, Biglari H. Phenol Removal from Aqueous Environment by Adsorption onto Pomegranate Peel Carbon. *Electron Physician.* 2016;8(11):3248-56. doi: [10.19082/3248](https://doi.org/10.19082/3248).
- Shahbazi R, Payan A, Fattahi M. Preparation, evaluations and operating conditions optimization of nano  $\text{TiO}_2$  over graphene based materials as the photocatalyst for degradation of phenol. *J Photochem Photobiol A Chem.* 2018;364:564-76. doi: [10.1016/j.jphotochem.2018.05.032](https://doi.org/10.1016/j.jphotochem.2018.05.032).
- Ahmed S, Rasul MG, Martens WN, Brown R, Hashib MA. Heterogeneous photocatalytic degradation of phenols in wastewater: A review on current status and developments. *Desalination.* 2010;261(1-2):3-18. doi: [10.1016/j.desal.2010.04.062](https://doi.org/10.1016/j.desal.2010.04.062).
- Zolfaghari A, Mortaheb HR, Meshkini F. Removal of N-Methyl-2-pyrrolidone by Photocatalytic Degradation in a Batch Reactor. *Ind Eng Chem Res.* 2011;50(16):9569-76. doi: [10.1021/ie200702b](https://doi.org/10.1021/ie200702b).
- Rauf MA, Meetani MA, Hisaindee S. An overview on the photocatalytic degradation of azo dyes in the presence of  $\text{TiO}_2$  doped with selective transition metals. *Desalination.* 2011;276(1-3):13-27. doi: [10.1016/j.desal.2011.03.071](https://doi.org/10.1016/j.desal.2011.03.071).
- Delsouz Khaki MR, Shafeeyan MS, Abdul Raman AA, Wan Daud WMA. Application of doped photocatalysts for organic pollutant degradation - A review. *J Environ Manage.* 2017;198(Pt 2):78-94. doi: [10.1016/j.jenvman.2017.04.099](https://doi.org/10.1016/j.jenvman.2017.04.099).
- Lam SM, Sin JC, Abdullah AZ, Mohamed AR. Photocatalytic  $\text{TiO}_2/\text{Carbon Nanotube Nanocomposites}$  for Environmental Applications: An Overview and Recent Developments. *Fullerenes, Nanotubes and Carbon Nanostructures.* 2014;22(5):471-509. doi: [10.1080/1536383X.2012.690458](https://doi.org/10.1080/1536383X.2012.690458).
- Zhang J, Vasei M, Sang Y, Liu H, Claverie JP.  $\text{TiO}_2/\text{Carbon}$  Photocatalysts: The Effect of Carbon Thickness on Catalysis. *ACS Appl Mater Interfaces.* 2016;8(3):1903-12. doi: [10.1021/acsami.5b10025](https://doi.org/10.1021/acsami.5b10025).
- Asilturk M, Sener S.  $\text{TiO}_2$ -activated carbon photocatalysts: Preparation, characterization and photocatalytic activities. *Chem Eng J.* 2012;180:354-63. doi: [10.1016/j.cej.2011.11.045](https://doi.org/10.1016/j.cej.2011.11.045).
- Shavisi Y, Sharifnia S, Hosseini SN, Khadivi MA. Application

- of TiO<sub>2</sub>/perlite photocatalysis for degradation of ammonia in wastewater. *J Ind Eng Chem.* 2014;20(1):278-83. doi: [10.1016/j.jiec.2013.03.037](https://doi.org/10.1016/j.jiec.2013.03.037).
18. Saleh TA, Gupta VK. Photo-catalyzed degradation of hazardous dye methyl orange by use of a composite catalyst consisting of multi-walled carbon nanotubes and titanium dioxide. *J Colloid Interface Sci.* 2012;371(1):101-6. doi: [10.1016/j.jcis.2011.12.038](https://doi.org/10.1016/j.jcis.2011.12.038).
  19. Liu SX, Chen XY, Chen X. A TiO<sub>2</sub>/AC composite photocatalyst with high activity and easy separation prepared by a hydrothermal method. *J Hazard Mater.* 2007;143(1-2):257-63. doi: [10.1016/j.jhazmat.2006.09.026](https://doi.org/10.1016/j.jhazmat.2006.09.026).
  20. Tryba B, Morawski AW, Inagaki M. Application of TiO<sub>2</sub>-mounted activated carbon to the removal of phenol from water. *Appl Catal B.* 2003;41(4):427-33. doi: [10.1016/S0926-3373\(02\)00173-X](https://doi.org/10.1016/S0926-3373(02)00173-X).
  21. Martins AC, Cazetta AL, Pezoti O, Souza JRB, Zhang T, Pilau EJ, et al. Sol-gel synthesis of new TiO<sub>2</sub>/activated carbon photocatalyst and its application for degradation of tetracycline. *Ceram Int.* 2017;43(5):4411-8. doi: [10.1016/j.ceramint.2016.12.088](https://doi.org/10.1016/j.ceramint.2016.12.088).
  22. Tang SK, Teng TT, Alkarkhi AFM, Li Z. Sonocatalytic Degradation of Rhodamine B in Aqueous Solution in the Presence of TiO<sub>2</sub> Coated Activated Carbon. *APCBEE Procedia.* 2012;1:110-5. doi: [10.1016/j.apcbee.2012.03.019](https://doi.org/10.1016/j.apcbee.2012.03.019).
  23. Gar Alalm M, Tawfik A, Ookawara S. Enhancement of photocatalytic activity of TiO<sub>2</sub> by immobilization on activated carbon for degradation of pharmaceuticals. *J Environ Chem Eng.* 2016;4(2):1929-37. doi: [10.1016/j.jece.2016.03.023](https://doi.org/10.1016/j.jece.2016.03.023).
  24. Shan AY, Ghazi TIM, Rashid SA. Immobilisation of titanium dioxide onto supporting materials in heterogeneous photocatalysis: A review. *Appl Catal A Gen.* 2010;389(1-2):1-8. doi: [10.1016/j.apcata.2010.08.053](https://doi.org/10.1016/j.apcata.2010.08.053).
  25. Park IS, Choi SY, Ha JS. High-performance titanium dioxide photocatalyst on ordered mesoporous carbon support. *Chem Phys Lett.* 2008;456(4-6):198-201. doi: [10.1016/j.cplett.2008.03.026](https://doi.org/10.1016/j.cplett.2008.03.026).
  26. An HB, Yu MJ, Kim JM, Jin M, Jeon JK, Park SH, et al. Indoor formaldehyde removal over CMK-3. *Nanoscale Res Lett.* 2012;7(1):7. doi: [10.1186/1556-276x-7-7](https://doi.org/10.1186/1556-276x-7-7).
  27. Liu Y, Li Q, Cao X, Wang Y, Jiang X, Li M, et al. Removal of uranium (VI) from aqueous solutions by CMK-3 and its polymer composite. *Appl Surf Sci.* 2013; 285(Pt B):258-66. doi: [10.1016/j.apsusc.2013.08.048](https://doi.org/10.1016/j.apsusc.2013.08.048).
  28. Hu L, Dang S, Yang X, Dai J. Synthesis of recyclable catalyst-sorbent Fe/CMK-3 for dry oxidation of phenol. *Microporous Mesoporous Mater.* 2012;147(1):188-93. doi: [10.1016/j.micromeso.2011.06.015](https://doi.org/10.1016/j.micromeso.2011.06.015).
  29. Beirami S, Barzoki HR, Bahramifar N. Application of response surface methodology for optimization of trace amount of diazinon preconcentration in natural waters and biological samples by carbon mesoporous CMK-3. *Biomed Chromatogr.* 2017;31(5):e3874.
  30. Jun S, Joo SH, Ryoo R, Kruk M, Jaroniec M, Liu Z, et al. Synthesis of new, nanoporous carbon with hexagonally ordered mesostructure. *J Am Chem Soc.* 2000;122(43):10712-3.
  31. Zhou F, Yan C, Liang T, Sun Q, Wang H. Photocatalytic degradation of Orange G using sepiolite-TiO<sub>2</sub> nanocomposites: Optimization of physicochemical parameters and kinetics studies. *Chem Eng Sci.* 2018;183:231-9. doi: [10.1016/j.ces.2018.03.016](https://doi.org/10.1016/j.ces.2018.03.016).
  32. Lam SM, Sin JC, Mohamed AR. Parameter effect on photocatalytic degradation of phenol using TiO<sub>2</sub>-P25/activated carbon (AC). *Korean J Chem Eng.* 2010;27(4):1109-16. doi: [10.1007/s11814-010-0169-8](https://doi.org/10.1007/s11814-010-0169-8).
  33. Chiou CH, Juang RS. Photocatalytic degradation of phenol in aqueous solutions by Pr-doped TiO<sub>2</sub> nanoparticles. *J Hazard Mater.* 2007;149(1):1-7. doi: [10.1016/j.jhazmat.2007.03.035](https://doi.org/10.1016/j.jhazmat.2007.03.035).
  34. Jiang T, Zhang L, Ji M, Wang Q, Zhao Q, Fu X, et al. Carbon nanotubes/TiO<sub>2</sub> nanotubes composite photocatalysts for efficient degradation of methyl orange dye. *Particuology.* 2013;11(6):737-42. doi: [10.1016/j.partic.2012.07.008](https://doi.org/10.1016/j.partic.2012.07.008).
  35. Alvarez MA, Orellana-Garcia F, Lopez-Ramon MV, Rivera-Utrilla J, Sanchez-Polo M. Influence of operational parameters on photocatalytic amitrole degradation using nickel organic xerogel under UV irradiation. *Arab J Chem.* 2018;11(4):564-72. doi: [10.1016/j.arabjc.2016.10.005](https://doi.org/10.1016/j.arabjc.2016.10.005).
  36. Akbal F. Photocatalytic degradation of organic dyes in the presence of titanium dioxide under UV and solar light: Effect of operational parameters. *Environ Prog.* 2005;24(3):317-22. doi: [10.1002/ep.10092](https://doi.org/10.1002/ep.10092).
  37. Mangrulkar PA, Kamble SP, Joshi MM, Meshram JS, Labhsetwar NK, Rayalu SS. Photocatalytic degradation of phenolics by N-doped mesoporous titania under solar radiation. *Int J Photoenergy.* 2012;2012:1-10. doi: [10.1155/2012/780562](https://doi.org/10.1155/2012/780562).
  38. Kansal S, Kaur N, Singh S. Photocatalytic degradation of two commercial reactive dyes in aqueous phase using nanophotocatalysts. *Nanoscale Res Lett.* 2009;4(7):709-16. doi: [10.1007/s11671-009-9300-3](https://doi.org/10.1007/s11671-009-9300-3).
  39. Rafiee E, Noori E, Zinatizadeh AA, Zanganeh H. Photocatalytic degradation of phenol using a new developed TiO<sub>2</sub>/graphene/heteropoly acid nanocomposite: synthesis, characterization and process optimization. *RSC Adv.* 2016;6(99):96554-62. doi: [10.1039/C6RA09897E](https://doi.org/10.1039/C6RA09897E).
  40. Deng J, Chen YJ, Lu YA, Ma XY, Feng SF, Gao N, et al. Synthesis of magnetic CoFe<sub>2</sub>O<sub>4</sub>/ordered mesoporous carbon nanocomposites and application in Fenton-like oxidation of rhodamine B. *Environ Sci Pollut Res Int.* 2017;24(16):14396-408. doi: [10.1007/s11356-017-8941-5](https://doi.org/10.1007/s11356-017-8941-5).